

The Thermodynamic Casimir Effect in ^4He Films near T_λ : Monte Carlo Results

Alfred Hucht

*Theoretical Physics, University of Duisburg-Essen, 47048 Duisburg, Germany**

(Dated: September 12, 2007)

The universal finite-size scaling function of the critical Casimir force for the three dimensional XY universality class with Dirichlet boundary conditions is determined using Monte Carlo simulations. The results are in excellent agreement with recent experiments on ^4He Films at the superfluid transition and with available theoretical predictions.

PACS numbers: 68.35.Rh, 05.10.Ln, 05.50.+q, 64.60.Fr

Casimir forces are always present in nature when a medium with long-range fluctuations is confined to restricted geometries. The quantum mechanical Casimir effect was proposed theoretically 60 years ago by H. B. G. Casimir [1] and describes an attractive force between two conducting plates in vacuum, induced by the vacuum fluctuations of the electromagnetic field. Furthermore, Goldstone modes [2] and surface fluctuations [3] can give rise to Casimir forces. Near continuous phase transitions, long-range fluctuations of the order parameter lead to the analogous *thermodynamic* Casimir effect [4], which can change the thickness of critical liquid films [5]. In a series of papers, Garcia and Chan [6, 7] and Ganshin *et al.* [8] were able to measure the thinning of liquid ^4He films close to the λ -point due to the thermodynamic Casimir effect. They found a characteristic deep minimum (dip) in the film thickness just below the superfluid transition temperature T_λ . Using finite-size scaling methods, they accurately determined the scaling function $\vartheta(x)$ of the Casimir force, which is universal for given universality class and boundary conditions. For liquid ^4He films it is believed that the superfluid order parameter vanishes at both surfaces of the film, implying Dirichlet boundary conditions [9].

Unfortunately, a theoretical explanation of the strong dip and a determination of the scaling function $\vartheta(x)$ is still lacking. In Ref. [10], this is stressed as the main theoretical problem with respect to the explanation of the ^4He experiments. While field theoretical results [11, 12, 13] are restricted to temperatures $T \geq T_c$, Monte Carlo simulations are only available for periodic boundary conditions until now [14], as only in this case the used stress tensor representation of the Casimir force is applicable. Recent attempts [15, 16] to explain the strong dip within mean field theories only find qualitative agreement with the experiments, neglecting the non-critical contributions of Goldstone modes.

In this letter, I present a direct calculation of the Casimir force using Monte Carlo simulations of the classical XY model. This method requires the computation of the free energy of the system with high accuracy, which is a major challenge within Monte Carlo simulations. Fortunately, it turns out that the determination is greatly simplified by the fact that only the difference of two free

energies is needed, which goes to zero exponentially fast above T_c . The resulting finite-size scaling function is in excellent agreement with the experimental results [6, 7, 8] as well as with available theoretical predictions [2, 11, 17].

The Casimir force per unit area of a system with size $L_\parallel^{d-1} \times L_\perp$ ($L_\parallel \rightarrow \infty$) is defined as [18, 19]

$$\beta F_{\text{Cas}}(T, L_\perp) = -\frac{\partial f_{\text{ex}}(T, L_\perp)}{\partial L_\perp}, \quad (1)$$

where $f_{\text{ex}}(T, L_\perp)$ denotes the excess free energy

$$f_{\text{ex}}(T, L_\perp) = f(T, L_\perp) - L_\perp f_\infty(T) \quad (2)$$

of the system. Here $f(T, L_\perp)$ is the free energy per unit area of a film of thickness L_\perp , measured in units of $k_B T$, and $f_\infty(T)$ is the bulk free energy density. For large L_\perp and near T_c the Casimir force fulfills the scaling *ansatz* [32]

$$\beta F_{\text{Cas}}(T, L_\perp) \sim L_\perp^{-d} \vartheta(x) \quad (3)$$

with the universal finite-size scaling function $\vartheta(x)$ and the scaling variable

$$x = t \left(\frac{L_\perp}{\xi_0^+} \right)^{1/\nu} \underset{t \gtrsim 0}{\sim} \left(\frac{L_\perp}{\xi_\infty^+} \right)^{1/\nu}. \quad (4)$$

Here I introduced the reduced temperature $t = T/T_c - 1$ and the bulk correlation length

$$\xi_\infty^+(t) \sim \xi_0^+ t^{-\nu}, \quad (t > 0). \quad (5)$$

Note that the universal finite-size scaling function $\vartheta(x)$ depends on the boundary conditions in the L_\perp -direction.

We can directly calculate the Casimir force (1) by integration of the internal energy as follows: Let us define the ‘‘internal Casimir force’’

$$\beta F_{\text{int}}(T, L_\perp) = -\left(\frac{\partial u(T, L_\perp)}{\partial L_\perp} - u_\infty(T) \right) \quad (6)$$

with the internal energy per unit area in units of $k_B T$

$$u(T, L_\perp) = -T \frac{\partial f(T, L_\perp)}{\partial T} \quad (7)$$

and the corresponding bulk density $u_\infty(T)$. The quantity $\partial u(T, L_\perp)/\partial L_\perp$ is directly accessible in Monte Carlo simulations using $u = \langle \beta \mathcal{H} \rangle / L_\perp^2$, and the central difference quotient

$$\frac{\partial u(T, L_\perp)}{\partial L_\perp} \approx \frac{u(T, L_\perp + 1) - u(T, L_\perp - 1)}{2}. \quad (8)$$

The Casimir force is then obtained by integration

$$\beta F_{\text{Cas}}(T, L_\perp) = - \int_T^\infty \frac{d\tau}{\tau} \beta F_{\text{int}}(\tau, L_\perp). \quad (9)$$

By Eqs. (3) and (9), the internal Casimir force fulfills the scaling form

$$- \beta F_{\text{int}}(T, L_\perp) \sim (\xi_0^+)^{-1/\nu} L_\perp^{(\alpha-1)/\nu} \vartheta'(x) \quad (10)$$

with the universal finite-size scaling function $\vartheta'(x)$. Note that within the scaling regime, Eq. (10), the relative error of Eq. (8) is $\mathcal{O}(L^{1/\nu-2-d})$.

We now consider the isotropic XY model on a simple cubic lattice of size $L_\parallel \times L_\parallel \times L_\perp$ in three dimensions with periodic boundary conditions in the parallel directions. The Dirichlet boundary conditions in perpendicular direction are implemented by open boundary conditions, which are known to be equivalent at large length scales [20, 21], although alternative implementations are possible [22]. The Hamiltonian reads

$$\mathcal{H} = - \frac{J}{2} \sum_{\langle ij \rangle} \vec{s}_i \cdot \vec{s}_j, \quad (11)$$

where $J > 0$ is the ferromagnetic exchange interaction, \vec{s}_i are 2-component unit vectors at site i , and the sum is restricted to nearest neighbors on the lattice. The simulations were performed for several system sizes with fixed aspect ratios $\rho = L_\perp/L_\parallel = 1:8$ and $1:16$ using the standard Wolff cluster algorithm [23]. To calculate Eq. (8), systems with thicknesses $L'_\perp = L_\perp \pm 1$ at constant L_\parallel were simulated for every combination of L_\parallel and L_\perp . At least 10^5 Monte Carlo sweeps per data point were performed.

To calculate the Casimir forces, Eqs. (1) and (6), it is necessary to have an expression for the bulk internal energy density $u_\infty(T)$. This is achieved using a combination of direct simulations of a large cubic system ($L = 96$) with periodic boundary conditions and results of Cucchieri *et al.* [24]. They determined the scaling behavior of the internal energy and specific heat of the XY model (11) in the region $|t| < 0.015$, where finite-size effects arise, using the scaling *ansatz*

$$k_B T u_\infty(T) = \epsilon_{\text{ns}} + T_c t \left[C_{\text{ns}} + \frac{A^\pm}{\alpha} |t|^{-\alpha} \left(\frac{1}{1-\alpha} + \frac{c_1^\pm}{1-\alpha+\nu\omega} |t|^{\nu\omega} + \frac{c_2^\pm}{2-\alpha} t \right) \right]. \quad (12)$$

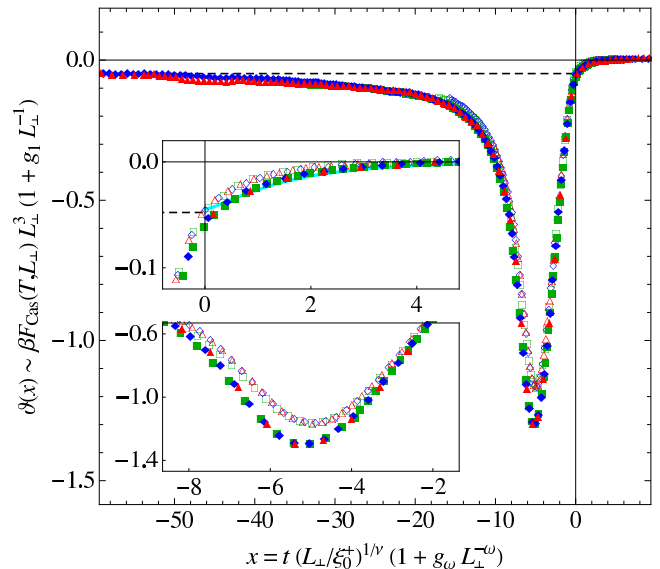


Figure 1: Results for the Casimir force using Eq. (14), for systems with $L_\perp = 8$ (green squares), $L_\perp = 12$ (blue diamonds), and $L_\perp = 16$ (red triangles), with aspect ratios $\rho = 1:8$ (open) and $\rho = 1:16$ (filled). The statistical error is of the order of the symbol size. The upper and lower insets are magnifications around $x = 0$ and around the minimum, respectively. Also shown are the Goldstone amplitude $-\zeta(3)/8\pi$ [2] (dashed line) and the field theoretical result [12] (cyan curve in upper inset). (color online)

The critical indices of the considered XY model are fixed to the values $\nu = 0.672(1)$, $\alpha = -0.017(3)$, $\omega = 0.79(2)$, $T_c/J = 2.20183(1)$, and $\xi_0^+ = 0.484(5)$ in the present letter, leading to the parameters $\epsilon_{\text{ns}} = -0.98841(3)$, $C_{\text{ns}} = 22.03$, $A^+ = 0.3790(8)$, $A^- = 0.3533(8)$, $c_1^+ = 0.015(1)$, $c_1^- = 0.109(2)$, $c_2^+ = -0.041(3)$, and $c_2^- = 0.211(4)$ [24]. For $|t| > 0.015$ finite-size effects are negligible; note that at $t = 0.015$ the correlation length, Eq. (5), has the value $\xi_\infty^+(0.015) \approx 8.1$, which is sufficiently small with respect to $L = 96$. While for periodic cubic systems the scaling corrections are moderate, systems with broken translational invariance and aspect ratios $\rho \ll 1$ show strong corrections to scaling. An analysis of usual thermodynamic quantities like the magnetic susceptibility $\chi(T, L_\perp)$ and the Binder cumulant $U(T, L_\perp)$ shows that it is necessary to use a modified scaling variable x (Eq. (4)) with Wegner corrections [25] of the form

$$x = t \left(\frac{L_\perp}{\xi_0^+} \right)^{1/\nu} (1 + g_\omega L_\perp^{-\omega}), \quad (13)$$

while the y -direction has rather small corrections for systems with constant ρ . However, for the numerical derivative with respect to L_\perp in (6) it is necessary to combine data of systems with $L'_\perp = L_\perp \pm 1$, leading to systems with different aspect ratio $\rho' \neq \rho$. This and the expected uncertainty of the numerical derivative itself introduces a scaling correction of the order $(1 + g_1 L_\perp^{-1})$ in the y -

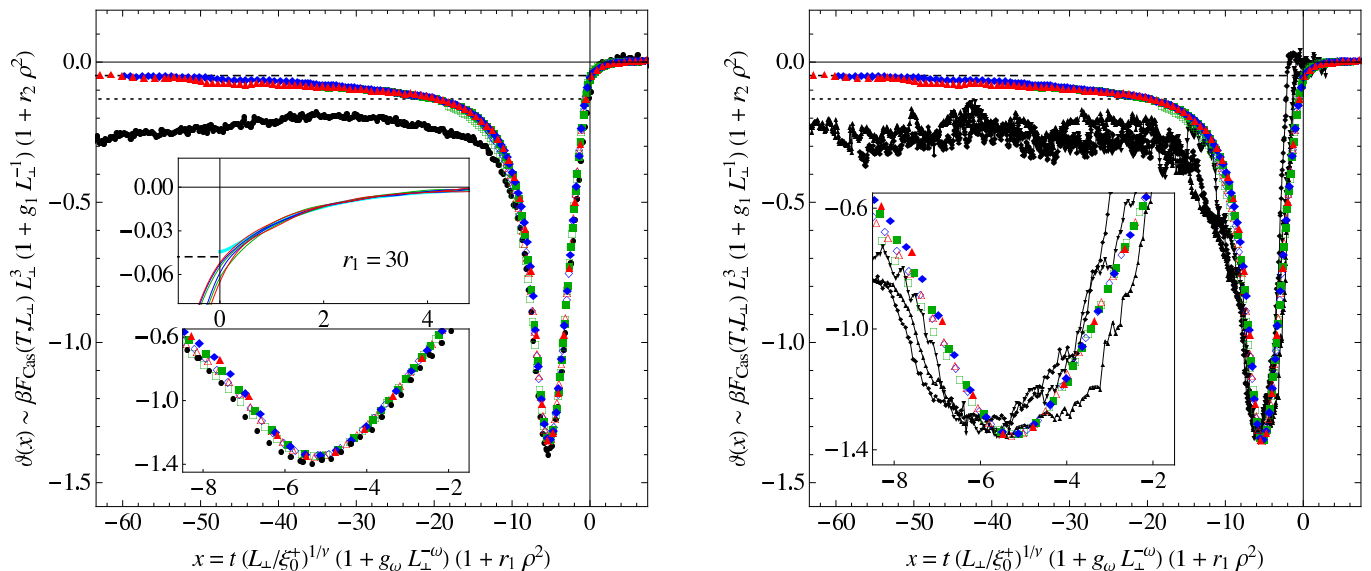


Figure 2: Universal finite-size scaling function $\vartheta(x)$ of the Casimir force for systems with $L_{\perp} = 8$ (green squares), $L_{\perp} = 12$ (blue diamonds), and $L_{\perp} = 16$ (red triangles), with aspect ratios $\rho = 1:8$ (open) and $\rho = 1:16$ (filled). The insets are magnifications of the respective regions. The results are compared (left) to the experimental data of Garcia and Chan [6, Cap. 1] (\bullet), as well as with the results (right) of Ganshin *et al.* [8] (\blacktriangle : 340Å, \blacklozenge : 285Å, \blacktriangledown : 238Å; solid lines are guides to the eye). Also shown are the Goldstone amplitude $-\zeta(3)/8\pi$ [2] (dashed line), the value $-11\zeta(3)/32\pi$ including surface fluctuations proposed in [3] (dotted line), and the field theoretical result [12] (cyan curve in left upper inset). (color online)

direction, leading to the final scaling *ansatz*

$$\beta F_{\text{Cas}}(T, L_{\perp}) \sim L_{\perp}^{-d} (1 + g_1 L_{\perp}^{-1})^{-1} \vartheta(x) \quad (14)$$

with x from Eq. (13).

The results for the Casimir force are shown in Figure 1 for six system sizes with $L_{\perp} \in \{8, 12, 16\}$, each with aspect ratio $\rho = 1:8$ and $\rho = 1:16$. It should be emphasized that the only fit parameters are the corrections to scaling amplitudes, $g_{\omega} = 2.0(1)$ and $g_1 = 5.5(2)$, which are adjusted [26] until the numerical data collapse onto a single curve, and that there is no free factor in neither x - nor y -direction. We can identify a slight dependence on the aspect ratio ρ in both directions. As the corrections due to the finite ρ are known to scale approximately with ρ^2 [27], a full data collapse can be achieved by adding a factor $(1 + r_1 \rho^2)$ to the x -axis and a factor $(1 + r_2 \rho^2)$ to the y -axis, with $r_1 = 4(1)$ and $r_2 = 10(1)$. Note that these corrections mainly shift the curves for $\rho = 1:8$, while the $\rho = 1:16$ curves are virtually unchanged within the error bars. The resulting scaling function is depicted in Figure 2, together with the results of Garcia and Chan [6] (left) as well as Ganshin *et al.* [8] (right). In the first case, only data for the thickest film with $d = 423$ Å are shown, which are regarded to have the highest quality [28], while the thinner films showed deviations in y -direction, presumably due to surface roughness [6, 8]. In order to compare the experimental data quantitatively with the present results, they are made dimensionless in x -direction using the measured correlation length amplitude $\xi_0^+ = 1.432$ Å of ^4He at T_{λ} [29], leading to a factor

$$(\xi_0^+)^{-1/\nu} = 0.586 \text{ \AA}^{-1/\nu}.$$

We find an excellent agreement within the error bars with both measurements for $x \gtrsim -8$. The universal amplitude of $\vartheta(x)$ at the minimum is $\vartheta(x_{\min}) = -1.35(3)$ at $x_{\min} = -5.3(1)$. These values agree with the values $x_{\min} = -5.4(1)$ of Garcia and Chan [6] and $\vartheta(x_{\min}) = -1.30(3)$ at $x_{\min} = -5.7(5)$ of Ganshin *et al.* [8]. It turns out that the overall agreement with [6] is even better than with [8], which might be attributed to the smaller fluctuations in y -direction in the data of [6], mainly visible below $x \approx -10$, and to the five times smaller error estimate in x -direction, clearly visible in the insets and at $x = 0$. For $x \lesssim -8$ we see an enhancement of the measured Casimir force not present in the calculated scaling function. This onset is weaker in the left figure. A possible explanation is the occurrence of surface fluctuations below this temperature, as proposed in [3]. At the critical point ($x = 0$) we find $\vartheta(0) = -0.047(2)$ [$-0.059(2)$] for $\rho = 1:8$ [$1:16$], which gives $\vartheta(0) = -0.062(5)$ for $\rho \rightarrow 0$. The resulting Casimir amplitude $\Delta = -0.031(3)$ agrees well with the estimate $\Delta = -0.03$ from [5, 27]. For $x \gtrsim 1$ the results nicely lie on the scaling function calculated by Krech and Dietrich [12] using renormalization group theory. Here $r_1 = 30$ was used, which again mainly shifts the data for $\rho = 1:8$, see upper inset in Figure 2(left). The quality of the used method, especially of the numerical integration, is demonstrated by the convergence of the calculated scaling function to the low temperature Goldstone value $\vartheta_{\text{Goldstone}} = -\zeta(3)/8\pi$ [2] for $x \rightarrow -\infty$ (dashed line in Figures 1 and 2).

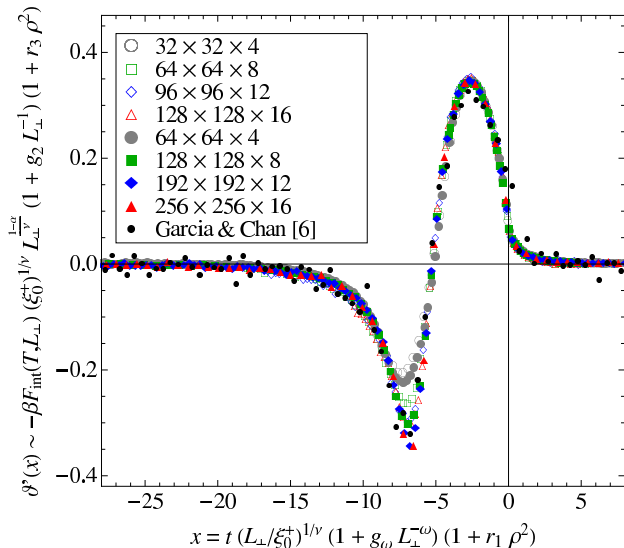


Figure 3: Universal finite-size scaling function $\vartheta'(x)$ of the internal Casimir force, Eq. (6), determined from eight different system sizes with aspect ratios $\rho = 1:8$ and $1:16$. The experimental results are obtained by binning (with $\Delta x = 0.5$) and numerical differentiation of the data from Garcia and Chan [6, Cap. 1]. (color online)

Figure 3 shows the results for the scaling function $\vartheta'(x)$ of the internal Casimir force, Eq. (6). The scaling plot contains data from eight system sizes with $L_{\perp} \in \{4, 8, 12, 16\}$, each with aspect ratio $\rho = 1:8$ and $\rho = 1:16$. While the aspect ratio correction in y -direction becomes $r_3 = r_2 - r_1$, the scaling correction g_2 cannot be expressed through g_{ω} and g_1 , as the corresponding L_{\perp} -exponents are different. The effective calculated value at $L_{\perp} \approx 10$ is $g_2 = 1.7$, which is modified to $g_2 = 2.0(2)$ to get the best data collapse. The results are compared to a numerical differentiation of the experimental data of Garcia and Chan [6, Cap. 1]. The results of Ganshin *et al.* [8] are not shown due to large fluctuations of the numerical derivative. The data collapse and the agreement with the experimental data is very convincing, also showing the small influence of statistical errors in the simulations. Only in the interval $-9 \lesssim x \lesssim -5$ we see higher order corrections to scaling, which are believed to stem from uncertainties in the numerical derivative, Eq. (8). However, these corrections only have small influence on the integrated Casimir force. Further work is necessary to clarify this behavior. Note that at the minimum of $\vartheta(x)$ we have $\vartheta'(x_{\min}) = 0$, which implies that $\lim_{L_{\perp} \rightarrow \infty} F_{\text{int}}(T_{\min}(L_{\perp}), L_{\perp}) = 0$ and

$$\left. \frac{\partial u(T, L_{\perp})}{\partial L_{\perp}} \right|_{T=T_{\min}(L_{\perp})} \sim u_{\infty}(T_{\min}(L_{\perp})), \quad (15)$$

i.e. at this temperature (and large L_{\perp}) the change in internal energy with L_{\perp} equals the corresponding bulk value. The connection (15) between the minimum of the

Casimir force and the internal energy shows that the shift of the minimum to negative x is a direct consequence of the strong shift in $T_c(L_{\perp})$ in systems with Dirichlet boundary conditions. This shift is also present in the exactly solvable two dimensional Ising model [18].

In summary, I determined the universal finite-size scaling function $\vartheta(x)$ of the Casimir force within the XY universality class with Dirichlet boundary conditions using Monte Carlo simulations. For sufficiently small aspect ratio $\rho = 1:16$ the results are in excellent agreement with the experimental results on ${}^4\text{He}$ by Garcia and Chan [6], and by Ganshin *et al.* [8], as well as with theoretical calculations for $T \geq T_c$ by Krech and Dietrich [11, 12]. The universal function $\vartheta(x)$ has a deep minimum at $x_{\min} = -5.3(1)$, with $\vartheta(x_{\min}) = -1.35(3)$. The results are in conformity with the assumption that the order parameter in ${}^4\text{He}$ asymptotically obeys Dirichlet boundary conditions. The method proposed in this letter has also been applied to systems with periodic boundary conditions [30], where a similar good agreement with available results [13, 14] is obtained. The application to other boundary conditions as well as to Ising and Heisenberg models is straightforward.

Note added in proof. Recently, Vasilyev *et al.* presented an alternative method to calculate $\vartheta(x)$ using Monte Carlo simulations [31].

I would like to thank Daniel Grüneberg, Hans Werner Diehl, Ralf Meyer, Daniel Dantchev, and Rafael Garcia for useful discussions and comments.

* Electronic address: fred<at>thp.Uni-DuE.de

- [1] H. B. G. Casimir, Proc. K. Ned. Akad. Wet., Ser. B, **51**, 793 (1948).
- [2] H. Li and M. Kardar, Phys. Rev. Lett. **67**, 3275 (1991).
- [3] R. Zandi, J. Rudnick, and M. Kardar, Phys. Rev. Lett. **93**, 155302 (2004), Note that due to an imprecision in [3] ($\Delta d \approx -1.85 \text{ \AA}$ instead of $\Delta d \approx -2.2 \text{ \AA}$ for the considered film) the deviation from experiment ($\Delta d_{\min} \approx -2.65 \text{ \AA}$) is nearly twice as large as reported, see Fig. 2(left).
- [4] M. E. Fisher and P.-G. de Gennes, C.R. Acad. Sc. Paris, Ser. B **287**, 209 (1972).
- [5] J. O. Indekeu, J. Chem. Soc. Faraday Trans. II **82**, 1835 (1986).
- [6] R. Garcia and M. H. W. Chan, Phys. Rev. Lett. **83**, 1187 (1999), URL <http://users.wpi.edu/~garcia/casimirdata/>.
- [7] R. Garcia and M. H. W. Chan, Phys. Rev. Lett. **88**, 086101 (2002).
- [8] A. Ganshin, S. Scheidemantel, R. Garcia, and M. H. W. Chan, Phys. Rev. Lett. **97**, 075301 (2006).
- [9] W. Huhn and V. Dohm, Phys. Rev. Lett. **61**, 1368 (1988).
- [10] D. Dantchev, M. Krech, and S. Dietrich, Phys. Rev. Lett. **95**, 259701 (2005).
- [11] M. Krech and S. Dietrich, Phys. Rev. Lett. **66**, 345 (1991), [Erratum: **67**, 1055 (1991)].
- [12] M. Krech and S. Dietrich, Phys. Rev. A **46**, 1922 (1992).

- [13] H. W. Diehl, D. Grüneberg, and M. A. Shpot, *Europhys. Lett.* **75**, 241 (2006).
- [14] D. Dantchev and M. Krech, *Phys. Rev. E* **69**, 046119 (2004).
- [15] R. Zandi, A. Shackell, J. Rudnick, M. Kardar, and L. P. Chayes, arXiv:cond-mat/0703262v2 (2007).
- [16] A. Maciołek, A. Gambassi, and S. Dietrich, arXiv:0705.1064v1 [cond-mat.stat-mech] (2007).
- [17] J. O. Indekeu, M. P. Nightingale, and W. V. Wang, *Phys. Rev. B* **34**, 330 (1986).
- [18] J. G. Brankov, D. M. Dantchev, and N. S. Tonchev, *Theory of Critical Phenomena in Finite-Size Systems – Scaling and Quantum Effects* (World Scientific, Singapore, 2000).
- [19] M. Krech, *Casimir Effect in Critical Systems* (World Scientific, Singapore, 1994).
- [20] H. W. Diehl, *Int. J. Mod. Phys. B* **11**, 3503 (1997).
- [21] C. Zhang, K. Nho, and D. P. Landau, *Phys. Rev. B* **73**, 174508 (2006).
- [22] N. Schultka and E. Manousakis, *Phys. Rev. Lett.* **75**, 2710 (1995).
- [23] U. Wolff, *Phys. Rev. Lett.* **62**, 361 (1989).
- [24] A. Cucchieri, J. Engels, S. Holtmann, T. Mendes, and T. Schulze, *J. Phys A: Math. Gen.* **35**, 6517 (2002).
- [25] F. Wegner, *Phys. Rev. B* **5**, 4529 (1972).
- [26] F. Hucht, *fsscale: A program for doing Finite-Size Scaling* (1998-2007), URL <http://www.thp.Uni-DuE.de/fsscale/>.
- [27] K. K. Mon and M. P. Nightingale, *Phys. Rev. B* **35**, 3560 (1987).
- [28] R. Garcia (2007), private communication.
- [29] W. Y. Tam and G. Ahlers, *Phys. Rev. B* **32**, 5932 (1985).
- [30] A. Hucht and D. Grüneberg (2007), in preparation.
- [31] O. Vasilyev, A. Gambassi, A. Maciołek, and S. Dietrich, arXiv:0708.2902v1 [cond-mat.stat-mech] (2007).
- [32] \sim means “asymptotically equal” in the respective limit, $L_{\perp} \rightarrow \infty$, $T \rightarrow T_c$, or both, keeping the scaling variable x fixed, e.g. $f(L) \sim g(L) \Leftrightarrow \lim_{L \rightarrow \infty} f(L)/g(L) = 1$